Polym. Bull. (2017) 74:4175–4194
DOI 10.1007/s00289-017-1954-x

ORIGINAL PAPER

Water absorption, residual mechanical and thermal properties of hydrothermally conditioned nano-Al_2O_3 enhanced glass fiber reinforced polymer composites

Ramesh Kumar Nayak[1] · **Bankim Chandra Ray**[2]

Received: 11 November 2016 / Revised: 15 February 2017 / Accepted: 16 February 2017 /
Published online: 23 February 2017

Abstract The durability of the nano-Al_2O_3 enhanced glass fiber reinforced polymer (GFRP) composites in hydrothermal environment is necessary for hydro/hygro thermal applications. The present investigation emphasizes the effect of nano-Al_2O_3 filler concentration on moisture absorption kinetics, residual mechanical and thermal properties of hydrothermally treated GFRP nano-composites. Nano-Al_2O_3 particles were mixed with epoxy matrix through temperature assisted magnetic stirrer and followed by ultrasonic treatment. It has been observed that, the addition of 0.1 wt% of nano-Al_2O_3 into the GFRP nano-composites reduces the moisture diffusion coefficient by 10%, as well as improves the flexural residual strength by 16% and interlaminar residual shear strength by 17% as compared to the neat epoxy GFRP composites. However, the glass transition temperature has not been improved by the addition of nano-Al_2O_3 filler. Weibull design parameters have been determined for dry and hydrothermally conditioned nano-composites. A good agreement between the experimental and the simulated stress–strain results has been observed. The interface failure mechanism has been evaluated by field emission scanning electron microscope to support the new findings.

Keywords Nano-Al_2O_3 · Hydrothermal · Water absorption · Flexural strength

✉ Ramesh Kumar Nayak
rnayakfme@kiit.ac.in

[1] School of Mechanical Engineering, KIIT University, Bhubaneswar, India

[2] Metallurgical and Materials Engineering, NIT Rourkela, Rourkela, India

Introduction

GFRP composites are one of the choices for the designing and the selection of materials in different engineering applications due to their high specific strength, better corrosion resistance and compatibility with other materials as compared to other metallic materials [1]. However, the long-term durability and performance of this class of material are of major concerns and resulting in hindrance to their wide applications. The micro/nano inorganic fillers are added to the epoxy matrix to improve the mechanical properties of the composites which can widen the application area of the materials. Inorganic nano fillers are more acceptable as potential fillers because of their low cost and easy fabrication method [2]. Researchers have found that micro-Al_2O_3 fillers improves fracture toughness, impact and flexural strength of carbon fiber reinforced polymer composites [3] and GFRP composites [4]. The thermo-mechanical properties are enhanced by incorporating CNT-Al_2O_3 hybrids in epoxy matrix [5]. The nano-Al_2O_3 particles improve bearing strength [6], storage modulus and glass transition temperature [7], flexural, thermal conductivity [8], Young's modulus [9], glass transition temperature, specific wear rate [10] and reduce the coefficient of thermal expansion [11]. Both nano and micro-Al_2O_3 particles at different proportions improve the mechanical properties [12].

Engineers and researchers have observed that the addition of micro/nano-Al_2O_3 fillers into the epoxy matrix improves the mechanical, thermo-mechanical, impact, fracture toughness, Young's modulus, wear, thermal conductivity and glass transition temperature. Nayak et al. [13]. have observed that addition of nano-Al_2O_3 particles into the epoxy matrix enhances the interlaminar shear strength. However, these materials are still facing challenges and threats at different environmental conditions like high and low temperature, water, alkaline, corrosive and UV light exposure. At high moisture/relative humidity or hydrothermal environment, polymer composites are susceptible to absorb moisture followed by degradation of their physical, thermal, electrical and mechanical properties. Absorbed moisture/water molecules are usually bonded with the hydroxyl group of epoxy and free water is clustered in the free volume/voids present inside the epoxy or at the matrix fiber interface [14, 15]. Water absorbed epoxy changes its properties both physically and chemically. Physical change of epoxy is basically plasticization and swelling. Chemical change of epoxy is chain scission and hydrolysis [16–19]. Glass transition temperature (T_g) of GFRP composites is affected by a physical change of epoxy. The mechanical properties are affected by the physical, chemical properties and the structure of the epoxy polymer. Overall, moisture absorption changes the thermo-physical, mechanical and chemical characteristics of FRP composites [20]. Another aspect of the degradation of mechanical properties is the ability of the matrix to microcrack under different environmental conditions [21–23]. Therefore, retention of the mechanical properties in a hydrothermal environment is critical and challenging to the design engineers and researchers.

One of the probable methods to improve the interface strength is by adding nano fillers into GFRP composites [24]. Inorganic (Al_2O_3, TiO_2, SiO_2, etc.) and carbon base (carbon Nano Tube, MCNT, SWCNT and graphene) nano fillers have been used to enhance the mechanical properties. Okhawilai et al. [25]. found that there is an improvement of modulus by 2.5 times with addition of nano-SiO_2 particles in epoxy-modified polybenzoxazine. Inorganic fillers/particles are combined with polymer matrix either dispersed form or mechanically contacted or chemically bonded or combination of two or all [26]. Micro cracks may deflect or pin or blunt at the nano particle surface during their propagation, resulting in the improvement of fracture toughness [27]. Therefore, the health of the interface or interphase determines the reliability and durability of the composites at different environmental conditions. It has been observed that nano-Al_2O_3, SiO_2 and TiO_2 particles reduce water permeability and affinity, resulting in the improvement of corrosion resistance and hydrolytic degradation of GFRP composites [28–30].

Although water absorption study is not surprising for GFRP composites, investigation of residual mechanical properties of nano-Al_2O_3 filled GFRP composites subjected to the acceleration of hydrothermal aging is quite interesting and necessary. Therefore, an attempt has been made to investigate the effect of nano-Al_2O_3 concentration on water absorption, residual mechanical and thermal properties of GFRP composites. Control GFRP and nano GFRP composites have been aged hydrothermally at 70 °C. The moisture diffusion coefficient has been determined with a comparison between the control and the nano GFRP composites. Residual mechanical and thermal properties have been evaluated for hydrothermally conditioned GFRP composites. Further Weibull design parameters have been determined for dry and hydrothermally conditioned composites. Experimental and Weibull simulated stress–strain results were compared. Nano and micro scale strengthening mechanism and failure modes of the composites have been analyzed through factrographic study using FESEM.

Materials and method

Materials

Control GFRP composites have been made using epoxy (Diglycidyl ether of Bisphenol A), hardener (Triethylene tetra amine) and woven roving E-glass fiber. Nano GFRP composites were made up of with nano-Al_2O_3 fillers at different wt%. Nano-Al_2O_3 particles have been procured from SRL Industries Limited, Mumbai, India. Some of the important properties of epoxy, E-glass fiber and nano particles have been reported in Table 1. The shape of the nano particles has been examined by field emission scanning electron microscope, shown in Fig. 1a. It has been observed that nano particles are almost spherical in shape. Nano-Al_2O_3 filler has been characterized by X-ray diffraction (XRD). A Bruker D8 advance XRD system was used for XRD analysis of the samples. Co Kα source and a Lynxeye 1D detector were used in the XRD system. Figure 1b shows the XRD patterns of nano Al_2O_3 filler.

Table 1 Properties of raw materials [30, 31]

Properties	Epoxy	$Al_2O_3(\alpha)$	Glass fiber
Density g/cm^3	1.15	3.90	2.58
Tensile strength (MPa)	70	260	3800
Tensile modulus (GPa)	3.6	370	78
Poisson's ratio	0.30	0.21	0.20

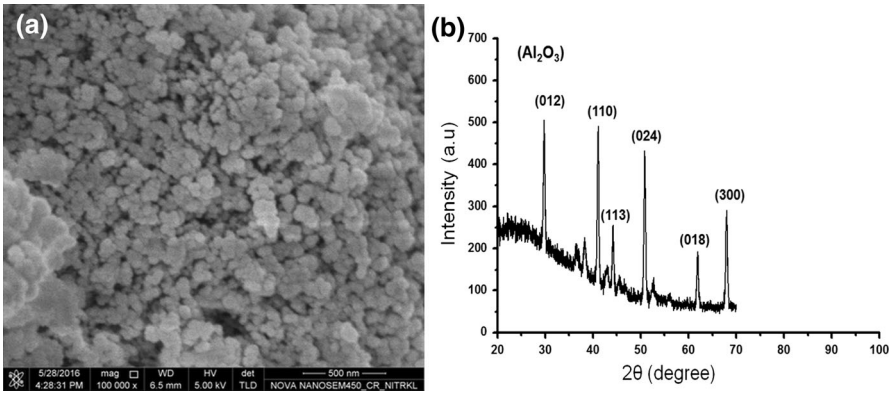

Fig. 1 FE-SEM images of nano Al_2O_3 particles **a** shape and **b** XRD analysis for Al_2O_3 (intensity versus 2θ)

Fabrication of control and nano GFRP composites

Nano-Al_2O_3 particles were dried at 100 °C for 2 h before mixing with epoxy resin. Control GFRP composite was fabricated without nano fillers. However, nano GF composites were fabricated with nano-Al_2O_3 filler at different concentrations. The weight fraction of fiber and epoxy was maintained at 60:40 ratios by weight for all composites. Each laminate contains 16 layers of woven roving glass fiber. Figure 2 shows the schematic diagram of the fabrication method of nano GFRP composites. The epoxy and nano-Al_2O_3 were stirred by a magnetic stirrer for 1 h, followed by sonication with a high frequency sonicater at 60 °C. Ash et al. [31] have used sonication method to disperse the nano-Al_2O_3 fillers in polymethyl methacrylate polymer to enhance the mechanical properties of the nano composites. The hardener amount is 10 wt% of epoxy and it is as per the supplier's instruction. Laminates were fabricated by a combination of hand lay-up method followed by temperature assisted compression molding (10 kg/cm^2 pressure, 60 °C and 20 min). Curing of control and nano GFRP composites was carried out at 140 °C for 6 h followed by furnace cooling. Cured GFRP composite laminates were cut at different sizes as per ASTM standard using diamond coated tipped cutter for characterization.

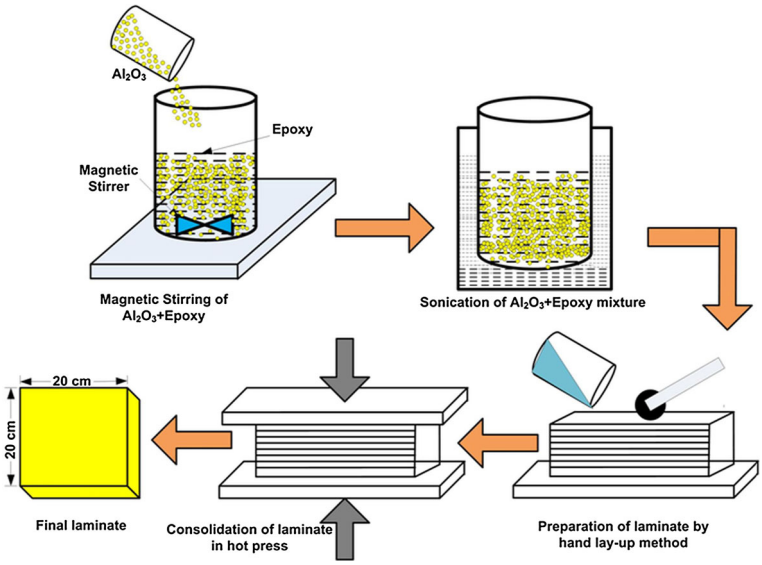

Fig. 2 Schematic view of the fabrication of nano Al_2O_3 filled GFRP composites

Results and discussions

Void content

Void content in the composites plays an important role on water absorption kinetics and mechanical properties of GFRP composites. The fiber wt% and the volume fraction of void have been determined by resin burn off test and as per ASTM D 3171-99 standard. As per the standard, six numbers of samples each with surface area 25 mm × 25 mm were taken into account for this analysis. Initial weight and dimensions of the samples were measured through high accuracy weighing balance and digital vernier caliper, respectively. Composites samples were put inside the muffle furnace at 575 ± 10 °C for 5 h to burn off the epoxy. Mathematical expression used to determine the void content is expressed in Eq. 1 [32, 33],

$$V_v = 1 - \rho_c \left(\frac{w_f}{\rho_f} + \frac{w_m}{\rho_m} \right), \tag{1}$$

where V_v is the volume fraction of void, ρ_c is the density of composites, ρ_f is the density of fiber, ρ_m is the density of epoxy matrix, w_f weight fraction of fiber, and w_m weight fraction of the epoxy matrix. Figure 3 shows the fiber wt% and void content of control and nano GFRP composites. It has been observed that the fiber weight percentage is slightly increased after fabrication and this may be because of the drain out of the epoxy during compression molding. The void content of the control GFRP is less as compared to the nano composites. This may be because of entrapped gases accumulated during magnetic stirring and sonication was not

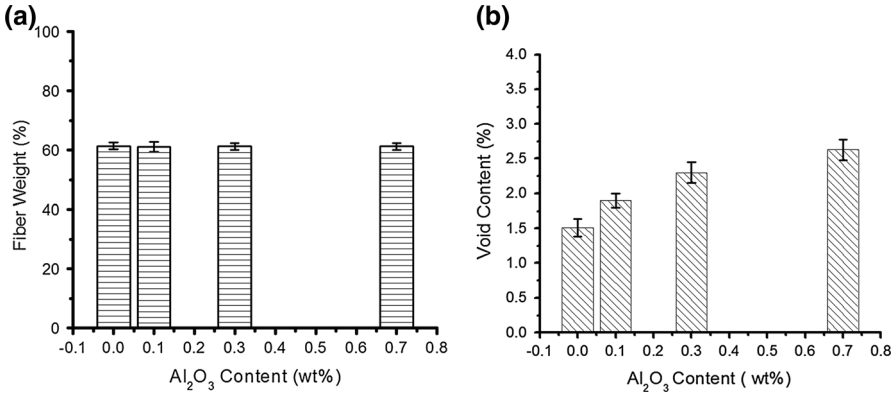

Fig. 3 **a** Fiber weight% and **b** void content in the composites versus Al_2O_3 content (wt%)

removed fully during compression molding. Similar observation is also reported by Nayak et al. [32].

Water diffusion kinetics

Control and nano-GFRP composite samples were dried properly at 100 °C for 5 h. The weight of the samples was measured by a high precision weighing machine. The samples were immersed into a temperature controlled water bath. Hydrothermal aging has been done at 70 °C for 30 days. The pH of water was measured and found around 5.65. There are six samples of each type which were immersed into the water bath. The samples were removed from the water bath in a regular interval of time. The adhered water on the surface of the composites were wiped off using tissue paper/cotton cloth and weighed with high precision weighing balance. The precaution has been taken to reduce the time required for removal of samples from water bath and till end of the weight measurement.

The amount of water absorbed by the composites (M_t) has been computed using the given Eq. (2), where M_t is the percentage of the moisture content at time t, m_0 is the weight of the specimen at its dry state and m is the specimen weight at time t. A typical water absorption behavior of GFRP composites is shown in Fig. 4. It has been observed that initially the nature for the water absorption by the polymer matrix is linear in nature and follows Fick's law of diffusion. Afterwards, the absorption is nearly saturated and become ceased after a certain time period. Again, it increases with increases in time. This is because of the degradation of epoxy and moisture penetrated through the micro cracks:

$$M_t = \frac{m - m_0}{m_0} \times 100\%. \tag{2}$$

The water/moisture diffusion coefficient is calculated in Fickian diffusion range using Eq. (3),

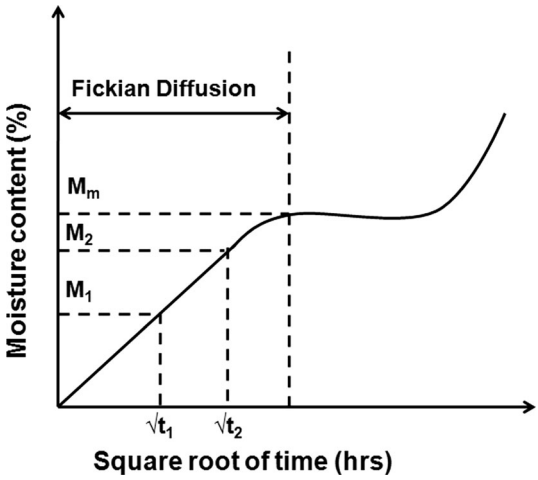

Fig. 4 The typical water absorption behavior of FRP composites [34]

$$D_z = \pi\left[\frac{h}{4 \times (\%M_m)}\right]^2 \times \left[\frac{(\%M_2 - \%M_1)}{\sqrt{t_2} - \sqrt{t_1}}\right]^2, \tag{3}$$

where h is the thickness of the sample, M_1, M_2 are the percentage of water absorption at time t_1 and t_2. In Eq. 3 D_z is one dimensional, which does not account for the diffusion taking place through the edge. Rao et al. [34], [35] suggested the corrected diffusion constant D, which is expressed in Eq. (4):

$$D = \frac{D_z}{\left[1 + \frac{h}{l} + \frac{h}{w}\right]^2}, \tag{4}$$

where l is the length of the sample, w is the width of the sample. Water diffusion coefficients have been measured for control and nano GF composites using the Eqs. 3 and 4. In this study, it is reasonable to assume that in the linear portion of the plot follows Fickian diffusion.

Figure 5a, b show the weight gain and diffusion coefficient versus nano-Al_2O_3 content (wt%) respectively. It is observed that the addition of 0.1 wt% of nano-Al_2O_3 reduces the water diffusion coefficient by 10% as compared to control and other nano GFRP composites. The decrease in the water absorption is attributed to the large surface area of nano-Al_2O_3 which may form a good interface bond between the matrix and the fiber as compared to the control GFRP composites. The improvement in the interface bond is also realized in the flexural and the ILSS test.

However, with the increase in the wt% of nano-Al_2O_3 (0.3 wt%), water absorption tendency increases. This is attributed to the uneven thermal expansion of epoxy (6.2×10^{-5} K^{-1}) [36], glass fiber ($5–12 \times 10^{-6}$ K^{-1}) [37], and nano-Al_2O_3 particles (8.1×10^{-6} K^{-1}) [38] which increases the diffusion through capillary action due to the matrix swelling and the microcracks formation at the interface. This is also because of more void content as compared to the control GFRP composites. With the addition of 0.7 wt% Al_2O_3, the diffusion coefficient further reduced. This may be because of more interface bond formed in comparison to the

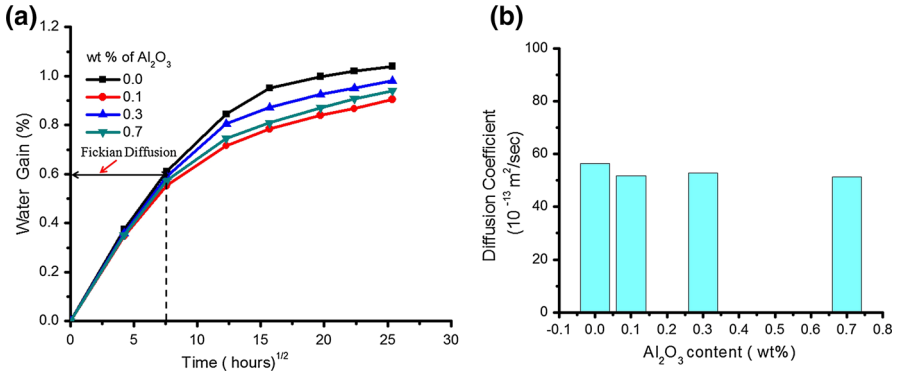

Fig. 5 **a** Water gain% versus square root of conditioning time **b** moisture diffusion coefficient as a function of nano-Al_2O_3 content (wt%)

isolated voids. Therefore, water diffusion through capillary action at the interface reduces and decreases the water diffusion coefficient. Composites having a higher amount of moisture content may degrade the mechanical, thermal (T_g), viscosity, and elasticity properties [35, 39].

Assessment of mechanical properties

Flexural strength

Durability and reliability of nano composites in the hydrothermal environment are very important to replace the metallic materials. Retainability of its interface strength and matrix toughness is very important for hydrothermal conditioned nano composites. The interface strength can be tailored through flexural test and it is evaluated as per ASTM D7264 standard. The span length of 72 mm has been maintained throughout the test. Universal Testing Machine (UTM) of INSTRON 5967 equipped with 5KN load cell was used to evaluate the mechanical properties at room temperature for both with and without hydrothermal conditioned nano composites at 1 mm/min cross head velocity.

Figure 6 shows the effect of nano filler content on flexural strength, strain and modulus. It is observed that the addition of 0.1 wt% of nano-Al_2O_3 to the epoxy matrix, flexural strength increases. A further increase in wt% of nano-Al_2O_3, reduces the flexural strength. This may attribute to the increase in wt% of nano filler, the increased tendency of agglomeration, reduction of the interface bond and formation of more number of isolated pores/voids in the GFRP composites. This leads to microcrack formation, resulting in flexural strength deterioration. However, flexural modulus improves with an increase in nano-Al_2O_3 content. Similar observation was also reported by Li et al. [5].

Figure 7 shows flexural residual strength and modulus versus nano-Al_2O_3 content. It is observed that the retention of flexural strength and modulus has been improved in nano composites in comparison to the control GFRP composites. The

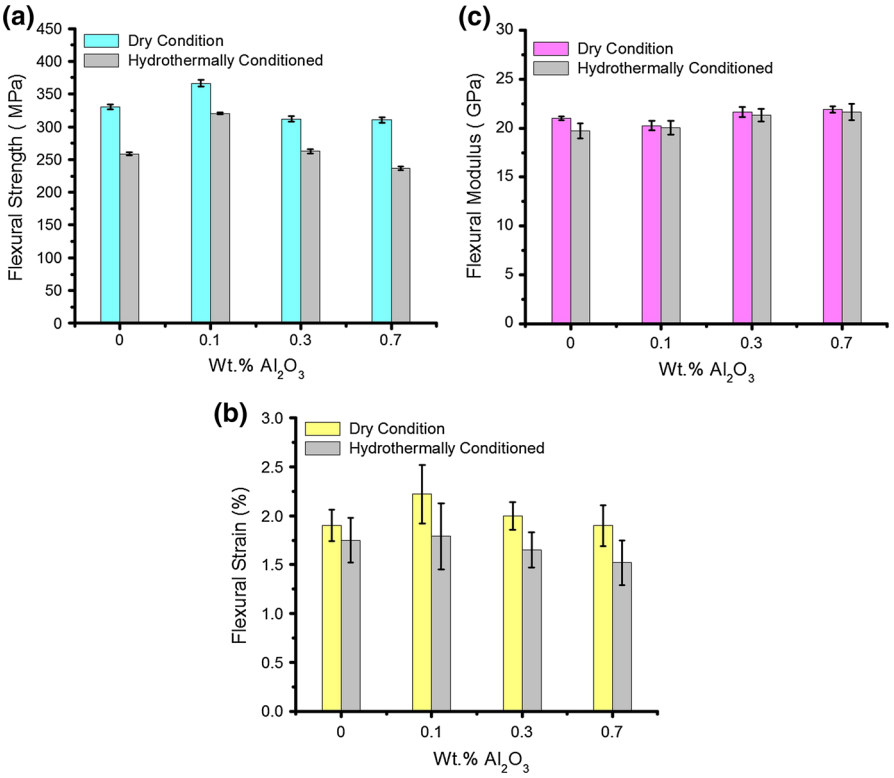

Fig. 6 **a** Flexural strength, **b** strain and **c** modulus of GFRP composites in dry and hydrothermal conditions versus nano-Al_2O_3 content

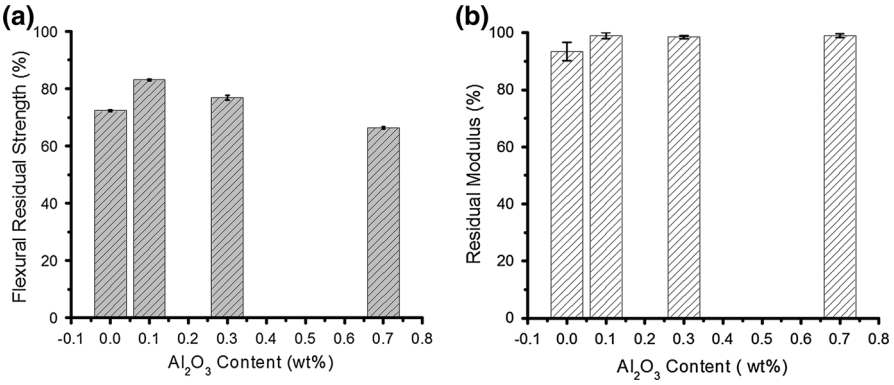

Fig. 7 Effect of nano-Al_2O_3 content on **a** flexural residual strength **b** residual modulus

maximum improvement of the flexural residual strength is about 16% and found in 0.1 wt% of nano-Al_2O_3 content of nano GFRP composites. This improvement of mechanical properties in hydrothermal condition attributes to the improvement of interface strength between the matrix and fiber, which reduces the diffusion of water

through capillary action of nano GFRP composites as compared to the control GFRP composites. With an increase in wt% of nano-Al_2O_3, mechanical properties deteriorated. This is because of weak inter-phase bonding between the resin and the nano fillers [7], more number of void formation and higher water diffusivity. However, there is a continuous improvement of flexural modulus with increase in the nano-Al_2O_3 content.

Prediction of Weibull design parameters

Fiber reinforced polymer composites have been used in different structural applications. Keeping in view of the reliability of the structural design, prediction of the mechanical properties through modeling and simulation is necessary. Fiber reinforced polymer (FRP) composites are anisotropic in nature and the mode of failure is dependent on the types of reinforcement, matrix and fiber/matrix interface strength. During deformation, each constituent of composites behaves differently either independently or combinedly depending on the flow behavior of the matrix. Therefore, statistical variation of mechanical performance has been addressed through Weibull probability distribution function to predict the mechanical properties of nano-Al_2O_3 filled GFRP composites. Weibull simulated stress (σ) $\sim$ strain (ε) relationship is expressed as per the Eq. (5) [40, 41],

$$\sigma = E\varepsilon \exp\left[-\left(\frac{E\varepsilon}{\sigma_0}\right)^{\beta}\right], \tag{5}$$

where E is the elastic modulus in the applied loading direction and σ_0, β are the Weibull design parameters. The physical significance of the Weibull design parameters of σ_0 and β is nominal strength and extent of randomness in the performance of the composites, respectively. Therefore, with the increase in the value of σ_0, the nominal strength of the composite increases and the randomness of the data reduce with increase in β. The design parameters can be determined by taking the double logarithm on both sides and rearrangement of the Eq. (5):

$$\ln\left[\ln\left(\frac{E\varepsilon}{\sigma}\right)\right] = \beta \ln(E\varepsilon) - \beta \ln(\sigma_0). \tag{6}$$

Using the experimental data of E, σ and ε, a straight line has been drawn, where the y axis is ln [ln ($E\varepsilon/\sigma$)] and x axis is ln ($E\varepsilon$). The slope of the straight line will become β and intercept $-\beta$ ln (σ_0). From the value of β and intercept $-\beta$ ln (σ_0), σ_0 has been calculated. Figure 8 shows the Weibull linear fitting of control and nano GFRP composites in dry and hydrothermal condition. A very good linear fitting of stress–strain curve and the R^2 value approaches to 1 has been observed. The design parameters for dry and hydrothermally conditioned samples have been reported in Table 2.

It is observed that with the increase in the experimental flexural strength, Weibull design parameter (σ_0) increases and similarly the randomness of the experimental data also decreases as the value of β increases. Using the calculated design

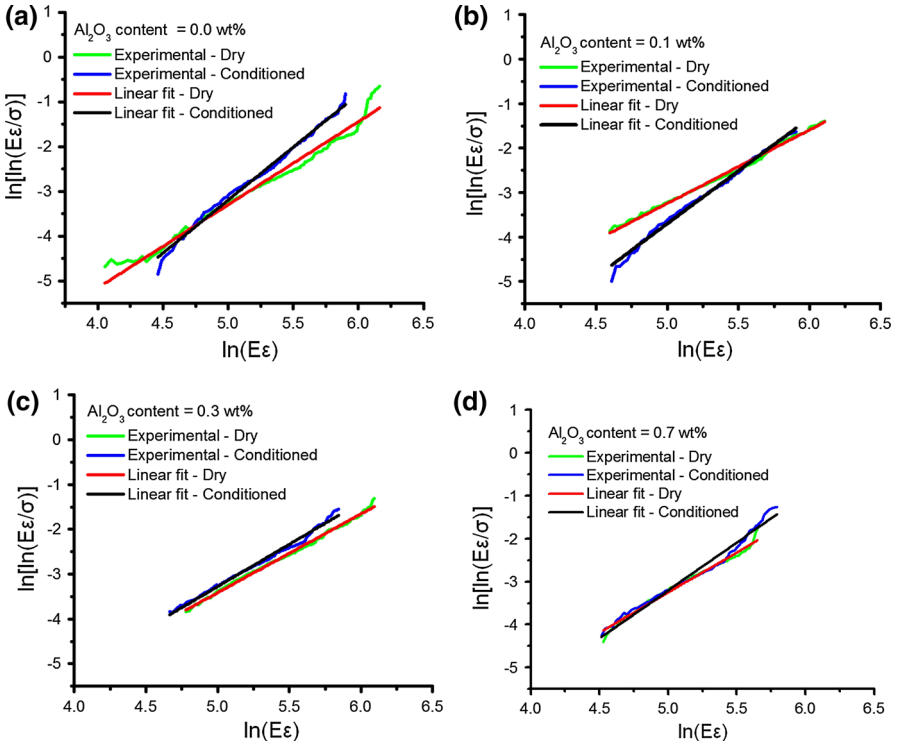

Fig. 8 Weibull linear fitting of dry and hydrothermal conditioned samples of nano-Al_2O_3 wt% **a** 0.0, **b**, 0.1, **c** 0.3, **d** 0.7

Table 2 Weibull design parameters of before and after hydrothermally conditioned composites

Al_2O_3 content (wt%)	σ_0		β	
	Dry	Conditioned	Dry	Conditioned
0	875.33 ± 18.50	571.50 ± 28.50	1.85 ± 0.10	2.36 ± 0.08
0.1	1050.66 ± 32.00	703.33 ± 21.50	1.95 ± 0.07	2.37 ± 0.12
0.3	908.16 ± 21.75	648.33 ± 11.50	1.89 ± 0.09	2.18 ± 0.04
0.7	845.33 ± 14.50	621.33 ± 20.50	1.86 ± 0.05	2.13 ± 0.17

parameters, Weibull simulated stress and strain is determined, and compared with the experimental one. Figure 9 shows a comparison between the experimental and the Weibull simulated stress–strain results for dry and hydrothermal conditioned composites at different wt% of nano-Al_2O_3 (a) 0.0 (b) 0.1 (c) 0.3 (d) 0.7. It is observed that there is a reasonable agreement between the experimental and the simulated stress–strain curve for both dry and hydrothermal conditioned composites. This indicates Weibull probability distribution function is very much helpful for prediction of flexural properties of nano fillers enhanced GFRP composites.

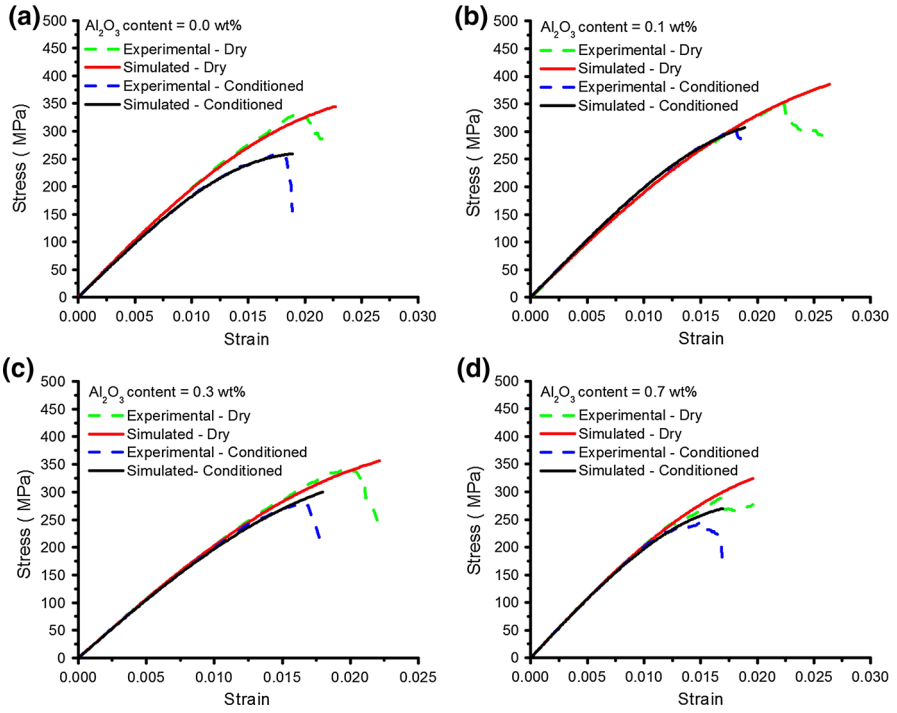

Fig. 9 Comparison between experimental and Weibull simulated stress–strain results for dry and hydrothermal conditioned samples at different wt% nano-Al_2O_3 **a** 0.0, **b** 0.1, **c** 0.3, **d** 0.7

Inter laminar shear strength

Interlaminar shear strength indicates the degree of adhesiveness between fiber and matrix of nano composites. Generally, nano fillers are added to improve the interface surface area between fiber and matrix to enhance the interface strength. Interface strength can be tailored through short beam shear test. In this investigation, a span length of 27 mm and cross head speed of 1 mm/min has been fixed throughout the test. All the tests have been performed at room temperature. Figure 10 shows interlaminar shear strength versus nano-Al_2O_3 content for dry and hydrothermally conditioned samples. It is seen that ILSS has been improved for both dry and hydrothermally conditioned samples in nano GFRP composites as compared to the control GFRP composites. The addition of 0.1 wt% of nano-Al_2O_3 in the epoxy matrix enhances 17% of residual ILSS as compared to the control GFRP composites. The improvement of ILSS is ascribed to the improvement of interface strength as compared to the reduction in micro-pores. Because, in the void content analysis, it is observed that there is an increase in void content % with increase in nano fillers concentration. The reduction in ILSS with an increase in Al_2O_3 content is attributed to the aggregation of nano-Al_2O_3 particles which reduce effective interface surface area resulting in decrease of interface shear strength. The decrease in ILSS of hydrothermally conditioned samples is attributed to microcrack

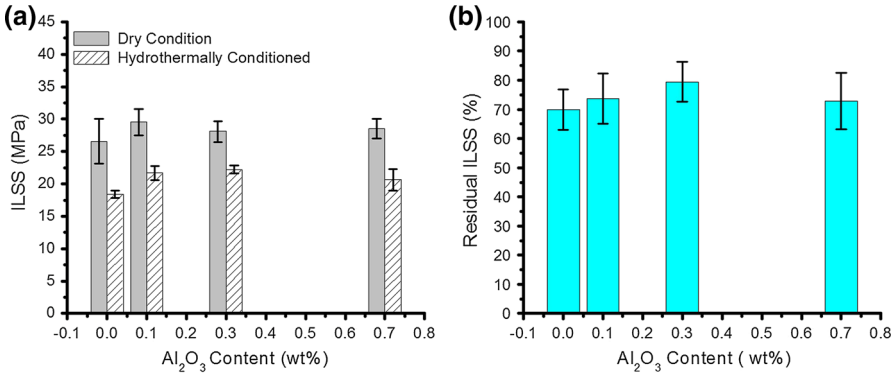

Fig. 10 **a** Interlaminar shear strength in dry and hydrothermally conditioned samples **b** residual interlaminar shear strength versus nano-Al_2O_3 content (wt%)

formation in the matrix, interphase and interfacial debonding. The microcrack formation at the interphase is due to the differential swelling of the matrix and fiber. This is because of the water absorption and thermal gradient during hydrothermal conditioning [21–23].

Factrographic study (FESEM)

Field emission scanning electron microscope (NOVA NANOSEM450) is used to investigate the mode of failure during flexural and ILSS test. Epoxy is non-conducting in nature and a thin platinum coating is coated on the fracture surface by sputtering method to get a conducting layer. Figure 11 shows different failure and strengthening mechanism involved during flexural and ILSS test in the dry condition. Figure 11a shows the matrix drainage and interfacial debonding of the composites having 0 wt% of nano-Al_2O_3, resulting in the decrease of flexural and ILSS strength as compared to other nano composites. Better interfacial bond, highly oriented shear cusps, zigzag dispersion of matrix, tough matrix and matrix deformation are the strengthening mechanisms which have been observed for the composites having 0.1 and 0.3 wt% of nano-Al_2O_3 (Fig. 11b, c). However, with further increase in the wt% of nano-Al_2O_3, both strengthening and weakening mechanisms have been observed in Fig. 11d, resulting decline in mechanical properties.

The improvement of the mechanical properties is attributed to the better dispersion of nano particles in the epoxy matrix, which increases the interface surface area leading to better bond between the matrix and the fiber. However, with the increase in nano-Al_2O_3 content, the probability of agglomeration increases and instead of nano effect, it will act as micro. This micro surface reduces the interface contact between matrix and fiber resulting in the decrease in interface dominated properties like flexural and interlaminar shear strength. The mode of failure undergoes different mechanism like matrix drainage, interfacial debonding, and

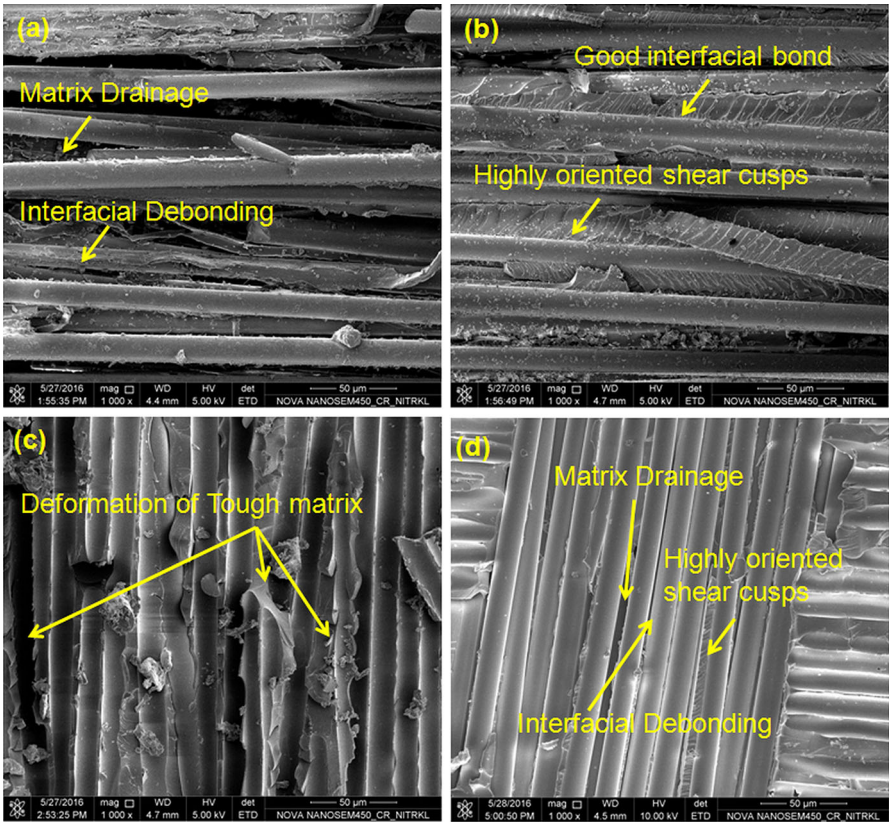

Fig. 11 Field Emission Scanning Electron Microscope images of a fractured surface of dry samples having different wt% of nano-Al_2O_3 **a** 0.0, **b** 0.1, **c** 0.3, **d** 0.7

matrix crack and fiber breakage. Similar observations are also reported by Li et al. [5].

Figure 12 shows the strengthening and failure mechanism of hydrothermally conditioned control and nano GFRP composites. Figure 12a shows smooth fiber imprints, micro void at the interface resulting in the decrease of flexural and interlaminar shear strength of control GFRP composites. However, with the addition of nano-Al_2O_3 (0.1 and 0.3 wt%), rough fiber imprints, hackles, severely deformed matrix and fiber breakage have been observed leading to the improvement of flexural and interlaminar shear strength [42]. This improvement of mechanical properties is attributed to better dispersion of nano particle which improves the interface area resulting in the good interface bond formation between the matrix and the fiber. During hydrothermal conditioning, absorbed water penetrated into the composites through micro voids, capillary action at the interface and also through micro channels. With a good interface bond, water absorption through capillary action is reduced and results in the improvement of the residual mechanical properties. However, further increase in the nano-Al_2O_3 content (0.7 wt%), matrix

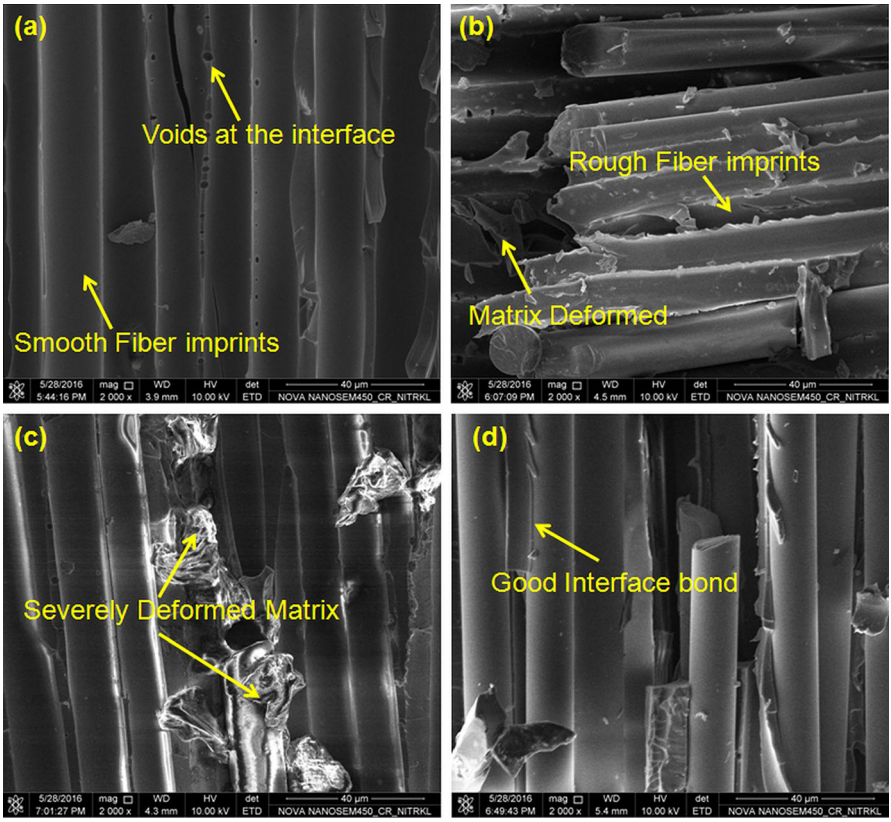

Fig. 12 FESEM images of fractured surface of hydrothermally conditioned samples having different wt% of nano-Al_2O_3 **a** 0.0, **b** 0.1, **c** 0.3, **d** 0.7

drainage, and interface debonding has been observed. Hence, overall mechanical properties have been deteriorating with an increase in wt% of nano-Al_2O_3.

Figure 13 shows the strengthening and undermined mechanism of the nano composites. At 0.1 wt% of nano-Al_2O_3, matrix toughening has been observed because of river line marks. However, micro voids have been observed for the composites having 0.7 wt% Al_2O_3 shown in Fig. 13b. From the void content analysis, it has been observed that with the increase in the nano-Al_2O_3, concentration, void percentage increases. Similarly, weight gain percentage increases with the increase in the nano filler content in hydrothermal treatment. Therefore, the micro voids act as the defects and the crack initiates at that defect location when it is subjected to some external load. Hence, instead of the positive effect of nano particles, it will contradict the nano effect on mechanical properties and resulting in undermined mechanical properties. Therefore, at higher concentration of nano fillers, the fabrication method of nano composites is critical to have a nano effect on mechanical properties.

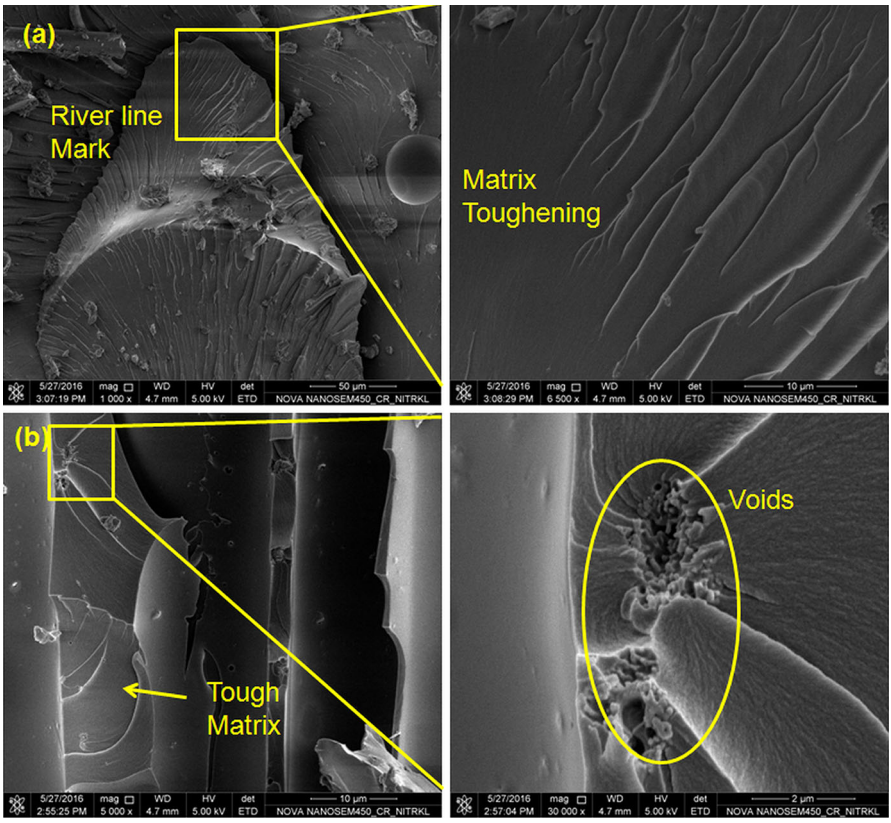

Fig. 13 Strengthening mechanism of nano composites **a** Al_2O_3 content 0.1 wt% and **b** aggregation of nano particles in the composites having nano-Al_2O_3 content 0.7 wt%

Thermal properties (glass transition temperature)

Thermal properties of nano composites are very critical in terms of the sustainability of the composites beyond a certain temperature, which can be evaluated and indicative through glass transition temperature. Differential scanning calorimetry (DSC-822, the Mettler Toledo) equipment has been used to determine and compare the glass transition temperature between control and nano GFRP composites. The test has been carried out under a nitrogen atmosphere and a heating rate of 10 °C/min. Figure 14 shows the glass transition temperature of control and nano GFRP composites of dry and hydrothermally conditioned samples. It is observed that the glass transition temperature has not been influenced by the addition of nano-Al_2O_3 fillers.

Figure 15a shows a comparison of glass transition temperature (T_g) between dry and hydrothermally conditioned samples and Fig. 15b shows the residual T_g. It is observed that T_g of hydrothermally aged control and nano GFRP composites has been decreased to around 30 °C. This means the thermal resistance of the nano

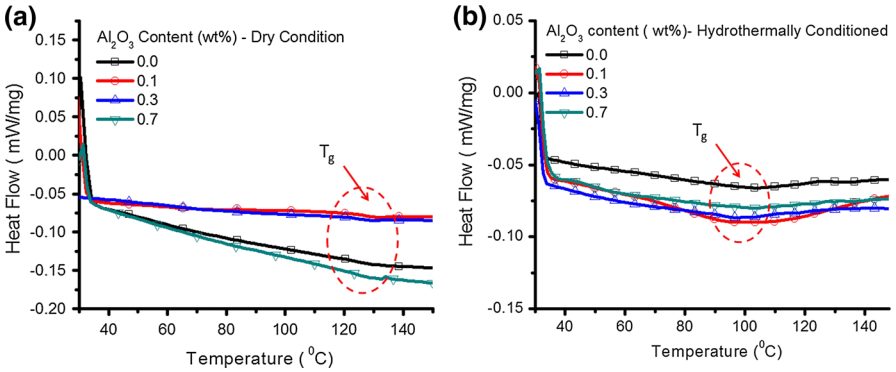

Fig. 14 Heat flow versus temperature of control GFRP and nano GFRP composites **a** dry, **b** hydrothermally conditioned

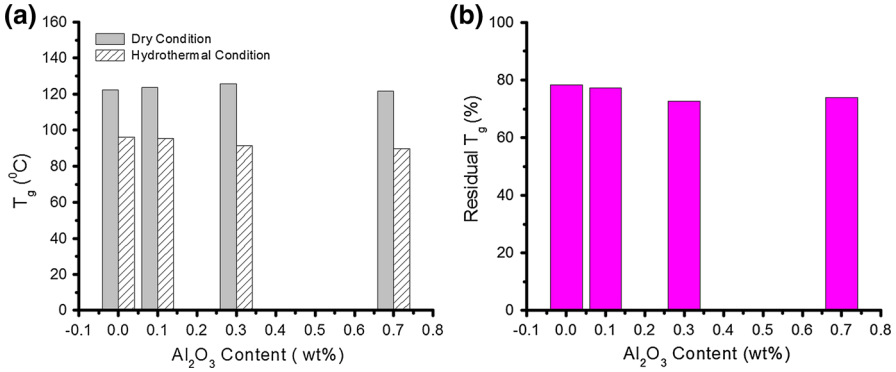

Fig. 15 Glass transition temperature of **a** dry and hydrothermally conditioned samples **b** residual T_g of hydrothermally conditioned nano composites

composites has not been improved. The decrease in T_g may be because of hydrolysis of epoxy which takes place during the hydrothermal conditioning leading to the decreasing cross linking density, which results in the decrease in T_g. However, hydrothermally conditioned nano composites reduce the T_g more as compared to control GFRP composites.

Conclusions

Effect of nano-Al_2O_3 concentration on mechanical and thermal properties has been evaluated for dry and hydrothermally conditioned GFRP nano-composites. The following conclusions are drawn:

1. The addition of 0.1 wt% of nano-Al_2O_3 into the control GFRP composites reduce moisture diffusion coefficient by 10% and improve residual flexural and interlaminar shear strength by 16 and 17%, respectively, as compared to the

control GFRP composites. However, with the increase in nano-Al_2O_3 content (weight%), modulus of the composites increases in both dry and hydrothermally conditioned composites.

2. The glass transition temperature has been reduced with increase in wt% of nano-Al_2O_3.
3. FESEM fractured surface revealed the enhancement of mechanical properties is because of the matrix toughening and the good interfacial bond between the matrix and the fiber. However, the mode of failure is the combination of the interface debonding, fiber pulls out, matrix cracking, matrix deformation and fiber breakage.
4. The reduction in the water absorption and the improvement of the residual mechanical properties of nano-Al_2O_3 filled GFRP composites create an opportunity to be employed in hydrothermal environment as compared to the control GFRP composites.

Acknowledgements The authors would like to thank the KIIT University, Bhubaneswar and NIT Rourkela for giving the opportunity to use the infrastructure and laboratory to carry out the research work.

References

1. Malvar LJ (1996) Literature review of durability of composites in reinforced concrete, Special Publication SP-2008-SHR. Naval Facilities Engineering Service Center, Port Hueneme, CA
2. Alexandre M, Dubois P (2000) Polymer-layered silicate nanocomposites: preparation, properties and uses of a new class of materials. Mater Sci Eng R Rep 28:1–63. doi:10.1016/S0927-796X(00)00012-7
3. Wang Z, Huang X, Bai L et al (2016) Effect of micro-Al_2O_3 contents on mechanical property of carbon fiber reinforced epoxy matrix composites. Compos Part B Eng 91:392–398. doi:10.1016/j.compositesb.2016.01.052
4. Nayak RK, Dash A, Ray BC (2014) Effect of epoxy modifiers (Al_2O_3/SiO_2/TiO_2) on mechanical performance of epoxy/glass fiber hybrid composites. Procedia Mater Sci 6:1359–1364. doi:10.1016/j.mspro.2014.07.115
5. Li W, Dichiara A, Zha J et al (2014) On improvement of mechanical and thermo-mechanical properties of glass fabric/epoxy composites by incorporating CNT–Al_2O_3 hybrids. Compos Sci Technol 103:36–43. doi:10.1016/j.compscitech.2014.08.016
6. Asi O (2010) An experimental study on the bearing strength behavior of Al_2O_3 particle filled glass fiber reinforced epoxy composites pinned joints. Compos Struct 92:354–363. doi:10.1016/j.compstruct.2009.08.014
7. Omrani A, Rostami AA (2009) Understanding the effect of nano-Al_2O_3 addition upon the properties of epoxy-based hybrid composites. Mater Sci Eng A 517:185–190. doi:10.1016/j.msea.2009.03.076
8. Hu Y, Du G, Chen N (2016) A novel approach for Al_2O_3/epoxy composites with high strength and thermal conductivity. Compos Sci Technol 124:36–43. doi:10.1016/j.compscitech.2016.01.010
9. Moreira DC, Sphaier LA, Reis JML, Nunes LCS (2012) Determination of Young's modulus in polyester-Al_2O_3 and epoxy-Al_2O_3 nanocomposites using the Digital Image Correlation method. Compos Part Appl Sci Manuf 43:304–309. doi:10.1016/j.compositesa.2011.11.005
10. Shi G, Zhang MQ, Rong MZ et al (2004) Sliding wear behavior of epoxy containing nano-Al_2O_3 particles with different pretreatments. Wear 256:1072–1081. doi:10.1016/S0043-1648(03)00533-7
11. Jiang W, Jin F-L, Park S-J (2012) Thermo-mechanical behaviors of epoxy resins reinforced with nano-Al_2O_3 particles. J Ind Eng Chem 18:594–596. doi:10.1016/j.jiec.2011.11.140
12. Hussain M, Nakahira A, Niihara K (1996) Mechanical property improvement of carbon fiber reinforced epoxy composites by Al_2O_3 filler dispersion. Mater Lett 26:185–191. doi:10.1016/0167-577X(95)00224-3

13. Nayak RK, Rathore D, Routara BC, Ray BC (2016) Effect of nano Al_2O_3 fillers and cross head velocity on interlaminar shear strength of glass fiber reinforced polymer composite. Int J Plast Technol 1–11. doi:10.1007/s12588-016-9158-z
14. Gonon P, Sylvestre A, Teysseyre J, Prior C (2001) Combined effects of humidity and thermal stress on the dielectric properties of epoxy-silica composites. Mater Sci Eng B 83:158–164. doi:10.1016/S0921-5107(01)00521-9
15. Maggana C, Pissis P (1999) Water sorption and diffusion studies in an epoxy resin system. J Polym Sci Part B Polym Phys 37:1165–1182. doi:10.1002/(SICI)1099-0488(19990601)37:11<1165:AID-POLB11>3.0.CO;2-E
16. Verghese KNE, Hayes MD, Garcia K et al (1999) Influence of matrix chemistry on the short term, hydrothermal aging of vinyl ester matrix and composites under both isothermal and thermal spiking conditions. J Compos Mater 33:1918–1938. doi:10.1177/002199839903302004
17. De'Nève B, Shanahan MER (1993) Water absorption by an epoxy resin and its effect on the mechanical properties and infra-red spectra. Polymer 34:5099–5105. doi:10.1016/0032-3861(93)90254-8
18. Xiao GZ, Delamar M, Shanahan MER (1997) Irreversible interactions between water and DGEBA/DDA epoxy resin during hygrothermal aging. J Appl Polym Sci 65:449–458. doi:10.1002/(SICI)1097-4628(19970718)65:3<449:AID-APP4>3.0.CO;2-H
19. Ray BC (2006) Temperature effect during humid ageing on interfaces of glass and carbon fibers reinforced epoxy composites. J Colloid Interface Sci 298:111–117. doi:10.1016/j.jcis.2005.12.023
20. Yilmaz T, Sinmazcelik T (2009) Effects of hydrothermal aging on glass–fiber/polyetherimide (PEI) composites. J Mater Sci 45:399–404. doi:10.1007/s10853-009-3954-1
21. Gautier L, Mortaigne B, Bellenger V (1999) Interface damage study of hydrothermally aged glass-fibre-reinforced polyester composites. Compos Sci Technol 59:2329–2337. doi:10.1016/S0266-3538(99)00085-8
22. Hodzic A, Kim JK, Lowe AE, Stachurski ZH (2004) The effects of water aging on the interphase region and interlaminar fracture toughness in polymer–glass composites. Compos Sci Technol 64:2185–2195. doi:10.1016/j.compscitech.2004.03.011
23. Ellyin F, Maser R (2004) Environmental effects on the mechanical properties of glass-fiber epoxy composite tubular specimens. Compos Sci Technol 64:1863–1874. doi:10.1016/j.compscitech.2004.01.017
24. Fan XJ, Lee SWR, Han Q (2009) Experimental investigations and model study of moisture behaviors in polymeric materials. Microelectron Reliab 49:861–871. doi:10.1016/j.microrel.2009.03.006
25. Okhawilai M, Dueramae I, Jubsilp C, Rimdusit S (2015) Effects of high nano-SiO_2 contents on properties of epoxy-modified polybenzoxazine. Polym Compos. doi:10.1002/pc.23807
26. Kinloch AJ, Masania K, Taylor AC et al (2007) The fracture of glass-fibre-reinforced epoxy composites using nanoparticle-modified matrices. J Mater Sci 43:1151–1154. doi:10.1007/s10853-007-2390-3
27. Park H-K, Su-Jin L, Yoon-Jeong K et al (2007) Mechanical properties and microstructures of GFRP rebar after long-term exposure to chemical environments. Polym Polym Compos 15:403–408
28. Sharifi Golru S, Attar MM, Ramezanzadeh B (2014) Studying the influence of nano-Al_2O_3 particles on the corrosion performance and hydrolytic degradation resistance of an epoxy/polyamide coating on AA-1050. Prog Org Coat 77:1391–1399. doi:10.1016/j.porgcoat.2014.04.017
29. Zhao H, Li RKY (2008) Effect of water absorption on the mechanical and dielectric properties of nano-alumina filled epoxy nanocomposites. Compos Part Appl Sci Manuf 39:602–611. doi:10.1016/j.compositesa.2007.07.006
30. Shi H, Liu F, Yang L, Han E (2008) Characterization of protective performance of epoxy reinforced with nanometer-sized TiO_2 and SiO_2. Prog Org Coat 62:359–368. doi:10.1016/j.porgcoat.2007.11.003
31. Ash BJ, Rogers DF, Wiegand CJ et al (2002) Mechanical properties of Al_2O_3/polymethylmethacrylate nanocomposites. Polym Compos 23:1014–1025. doi:10.1002/pc.10497
32. Nayak RK, Mahato KK, Ray BC (2016) Water absorption behavior, mechanical and thermal properties of nano TiO_2 enhanced glass fiber reinforced polymer composites. Compos Part Appl Sci Manuf 90:736–747. doi:10.1016/j.compositesa.2016.09.003
33. Nayak RK, Mahato KK, Routara BC, Ray BC (2016) Evaluation of mechanical properties of Al_2O_3 and TiO_2 nano filled enhanced glass fiber reinforced polymer composites. J Appl Polym Sci 133. doi:10.1002/app.44274

34. Rao RMVGK, Chanda M, Balasubramanian N (1984) Factors affecting moisture absorption in polymer composites part ii: influence of external factors. J Reinf Plast Compos 3:246–253. doi:10.1177/073168448400300305
35. Pervin F, Zhou Y, Rangari VK, Jeelani S (2005) Testing and evaluation on the thermal and mechanical properties of carbon nano fiber reinforced SC-15 epoxy. Mater Sci Eng A 405:246–253. doi:10.1016/j.msea.2005.06.012
36. Huang CJ, Fu SY, Zhang YH et al (2005) Cryogenic properties of SiO_2/epoxy nanocomposites. Cryogenics 45:450–454. doi:10.1016/j.cryogenics.2005.03.003
37. Chu XX, Wu ZX, Huang RJ et al (2010) Mechanical and thermal expansion properties of glass fibers reinforced PEEK composites at cryogenic temperatures. Cryogenics 50:84–88. doi:10.1016/j.cryogenics.2009.12.003
38. Corundum, Aluminum Oxide, Alumina, 99.9%, Al_2O_3. http://www.matweb.com/search/DataSheet.aspx?MatGUID=c8c56ad547ae4cfabad15977bfb537f1&ckck=1. Accessed 11 Jun 2016
39. Tritt TM (2004) Thermal conductivity. Springer, US
40. Zhou Y, Pervin F, Lewis L, Jeelani S (2008) Fabrication and characterization of carbon/epoxy composites mixed with multi-walled carbon nanotubes. Mater Sci Eng A 475:157–165. doi:10.1016/j.msea.2007.04.043
41. Prusty RK, Rathore DK, Shukla MJ, Ray BC (2015) Flexural behaviour of CNT-filled glass/epoxy composites in an in situ environment emphasizing temperature variation. Compos Part B Eng 83:166–174. doi:10.1016/j.compositesb.2015.08.035
42. Kim H-Y, Park Y-H, You Y-J, Moon C-K (2008) Short-term durability test for GFRP rods under various environmental conditions. Compos Struct 83:37–47. doi:10.1016/j.compstruct.2007.03.005